Comprehensive study of the metal/semiconductor character of adatom-induced Ag/Si(111) reconstructions

H. M. Zhang,* Kazuyuki Sakamoto, and R. I. G. Uhrberg
Department of Physics and Measurement Technology, Linköping University, S-581 83 Linköping, Sweden
(Received 13 August 2001; published 7 December 2001)

A $\sqrt{21}\times\sqrt{21}$ reconstruction can be formed by either Ag or Au adsorption on the Ag/Si(111) $\sqrt{3}\times\sqrt{3}$ surface. The electronic structures determined by angle-resolved photoemission from these two $\sqrt{21}\times\sqrt{21}$ surfaces show clear similarities. The presence of the extra Ag or Au adatoms results in a metallic surface with two surface state bands near the Fermi level. Only one of these bands crosses the Fermi level instead of two as reported in the literature. A tiny amount of Ag deposited onto the $\sqrt{21}\times\sqrt{21}$-Ag surface below 100 K transforms it into a 6×6 periodicity. The additional Ag leads to an interesting transition from the metallic $\sqrt{21}\times\sqrt{21}$ surface to a semiconducting 6×6 surface with a gap of about 0.2 eV with respect to the Fermi level.

DOI: 10.1103/PhysRevB.64.245421 PACS number(s): 68.35.−p, 73.20.−r, 79.60.−i

Presently, the surface electronic structure around the Fermi level of different semiconductor surfaces attracts a lot of attention. Many studies focus on phase transitions on two- and one-dimensional systems and the possible occurrence of a metal to semiconductor transition. When the temperature is lowered a Peierls or a charge density wave transition may take place resulting in a gap opening. Another interesting type of metal/semiconductor transition is related to the presence of a small amount of additional adatoms. We have recently reported that the Ag/Ge(111) system shows a metal to semiconductor transition when Ag atoms are added to the Ag/Ge(111) $\sqrt{39}\times\sqrt{39}$ surface to form the 6×6 phase.[1] The Ag/Si(111) system, which has been subject to extensive studies, shows a $\sqrt{21}\times\sqrt{21}$ and a 6×6 reconstruction. The basic character of the reconstructions formed by Ag on the Si(111) and Ge(111) surfaces is very similar although different periodicities are observed for the intermediate phases. The observation of the metal to semiconductor transition on Ag/Ge(111), has motivated us to perform a detailed study of the surface electronic structure near the Fermi level (E_F) for the three different periodicities of the Ag/Si(111) system. Information about the surface electronic structure is especially important when the surface conductance is studied. This topic has been discussed quite a lot in the literature in connection to the Ag/Si(111) surfaces since a strong variation is observed when the reconstruction changes.

The Ag/Si(111) $\sqrt{3}\times\sqrt{3}$ surface, which is formed by annealing a Si(111) surface covered by 1 monolayer (ML) of Ag adatoms, seems to be well described by the honeycomb-chain-trimer (HCT) model.[2] The $\sqrt{21}\times\sqrt{21}$ and the 6×6 phases are formed by adding Ag to the $\sqrt{3}\times\sqrt{3}$ surface below room temperature.[3,4] The electronic structures of the Ag-induced $\sqrt{21}\times\sqrt{21}$ and 6×6 phases have not been reported so far. All the available photoemission data on the surface electronic structure of the $\sqrt{21}\times\sqrt{21}$ phase come from the closely related Au- and Cu-induced $\sqrt{21}\times\sqrt{21}$ surfaces. It has been reported that the $\sqrt{3}\times\sqrt{3}$ phase of Ag/Si(111) shows one metallic band,[5,6] while two metallic bands have been reported for the Au- and Cu-induced $\sqrt{21}\times\sqrt{21}$ surfaces.[4,6–8] The presence of the metallic band of the $\sqrt{3}\times\sqrt{3}$ surface can be explained in terms of an adatom induced partial occupation of a surface state band that should be unoccupied for an ideal $\sqrt{3}\times\sqrt{3}$ surface.[2,5] There are two natural sites for the Ag adatoms, i.e., Ag trimer or Si trimer sites. Adsorption of Ag on Ag trimer sites is, however, supported by theoretical calculations,[9] which find these sites to be more favorable, energetically, than the Si trimer sites. These calculations were performed for 1/3 ML of Ag which means that all Ag trimers were occupied and that the surface still had a $\sqrt{3}\times\sqrt{3}$ periodicity. Two metallic surface bands were found which both cross the Fermi level. It was concluded that the upper band is an adatom-induced band, while the lower band is derived from the underlying $\sqrt{3}\times\sqrt{3}$ surface. The anomalously high conductance value observed for the $\sqrt{21}\times\sqrt{21}$ was explained in terms of these two metallic bands,[4,6–10] which were believed to exist also on the Ag-induced $\sqrt{21}\times\sqrt{21}$ surface. The concept of two metallic surface bands on the $\sqrt{21}\times\sqrt{21}$ surface is, however, not consistent with our photoemission data as is shown below.

In this paper we present data from the Ag-induced $\sqrt{21}\times\sqrt{21}$ and 6×6 surfaces obtained by angle-resolved photoelectron spectroscopy (ARPES). Valence band spectra from the Au-induced $\sqrt{21}\times\sqrt{21}$ surface are also shown in order to facilitate a comparison with the Ag-induced one. The presence of the extra Ag/Au atoms results in a metallic surface with two surface state bands near the Fermi level. However, only one surface band on the $\sqrt{21}\times\sqrt{21}$ surface is metallic. Both the data obtained from the Ag-induced and the Au-induced $\sqrt{21}\times\sqrt{21}$ surfaces give the same picture. Further, addition of Ag onto the $\sqrt{21}\times\sqrt{21}$-Ag surface leads to an interesting transition from a metallic surface to a semiconducting 6×6 phase.

The photoemission study was performed at beam line 33 at the Max-I synchrotron radiation facility in Lund, Sweden. The angle-resolved valence band spectra presented here were obtained with a total energy resolution of $\sim$50 meV and an angular resolution of $\pm2°$. The Si(111) samples cut from a single crystal wafer (Sb doped, 3 Ω cm) were preoxidized by an etching method and cleaned in-situ by stepwise direct current heating up to 930 °C. This procedure resulted in a clean and well-ordered surface, as evidenced by the strong surface state emission and a sharp 7×7 low-energy electron

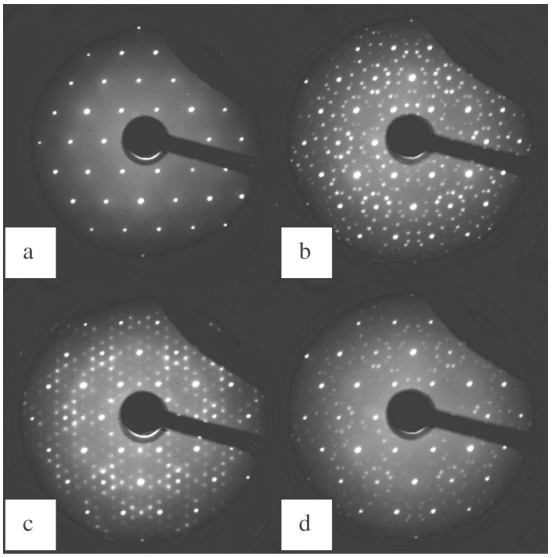

FIG. 1. LEED patterns obtained with a beam energy of 114 eV. (a) Ag/Si(111) $\sqrt{3}\times\sqrt{3}$ at 100 K with ~1.0 ML of Ag; (b) $\sqrt{21}\times\sqrt{21}$ surface at 100 K with ~0.15 ML of Ag added to the $\sqrt{3}\times\sqrt{3}$ surface; (c) 6×6 surface at 70 K with ~0.22 ML of Ag added to the $\sqrt{3}\times\sqrt{3}$ surface; (d) Au-induced $\sqrt{21}\times\sqrt{21}$ surface at 100 K with ~0.15 ML of Au added to the $\sqrt{3}\times\sqrt{3}$ surface.

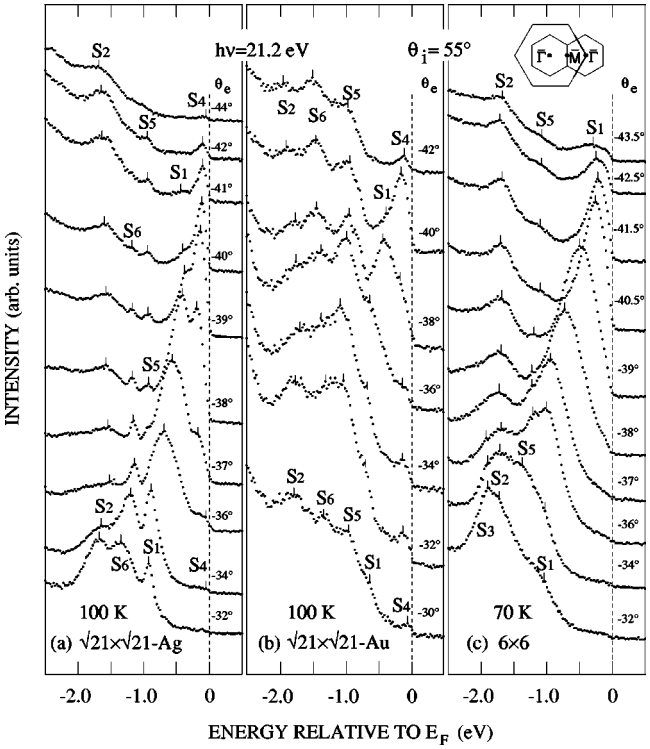

FIG. 2. ARPES spectra recorded from the Ag/Si(111) surfaces with a photon energy of 21.2 eV. The emission angles correspond to $k_{\|}$ points near the $\bar{\Gamma}$ point of the second $\sqrt{3}\times\sqrt{3}$ SBZ, along the $\bar{\Gamma}$-$\bar{M}$-$\bar{\Gamma}$ line (see inset). (a) $\sqrt{21}\times\sqrt{21}$ surface at 100 K; (b) Au-induced $\sqrt{21}\times\sqrt{21}$ surface at 100 K; (c) 6×6 surface at 70 K.

diffraction (LEED) pattern. Ag and Au were evaporated onto the Si sample from tungsten filament sources calibrated by a quartz crystal monitor. Evaporation of 1 ML of Ag followed by annealing at 520 °C for 2 min, resulted in a sharp $\sqrt{3}\times\sqrt{3}$ LEED pattern [Fig. 1(a)]. A $\sqrt{21}\times\sqrt{21}$ surface [Fig. 1(b)], which is visible by LEED at temperatures slightly below room temperature, was obtained by evaporating ~0.15 ML of Ag onto the $\sqrt{3}\times\sqrt{3}$ surface. The 6×6 surface [Fig. 1(c)] was formed either by adding ~0.22 ML of Ag onto the $\sqrt{3}\times\sqrt{3}$ surface, or by adding ~0.07 ML onto the $\sqrt{21}\times\sqrt{21}$ surface, below 100 K. The Au-induced $\sqrt{21}\times\sqrt{21}$ surface [Fig. 1(d)], which is visible by LEED at room temperature, was obtained by evaporating ~0.15 ML of Au onto the Ag/Si(111) $\sqrt{3}\times\sqrt{3}$ surface.

A set of angle-resolved photoemission spectra from the $\sqrt{21}\times\sqrt{21}$-Ag surface along the $\bar{\Gamma}$-$\bar{M}$-$\bar{\Gamma}$ line of the $\sqrt{3}\times\sqrt{3}$ SBZ is shown in Fig. 2(a). Both the $\sqrt{21}\times\sqrt{21}$ and the 6×6 reconstructions can be regarded as superstructures on a $\sqrt{3}\times\sqrt{3}$ substrate.[11–13] In similarity with the earlier studies we therefore use the $\sqrt{3}\times\sqrt{3}$ surface Brillouin zone (SBZ) to describe the azimuthal directions for all reconstructions. Six surface states S_1–S_6 were detected in the valence band spectra. All are present in Fig. 2(a), except for S_3, which appears for smaller emission angles. Two surface states, S_1 and S_4, are important for the discussion of the metallicity of the surface. S_4, which has a dispersion minimum at −0.19 eV at $\theta_e=-38°$, crosses E_F at $\theta_e=-34°$ and $\theta_e=-44°$ resulting in a clear metallic character of the surface. The S_1 surface state is located at −0.92 eV at $\theta_e=-32°$ and it disperses steeply upwards to a maximum energy of −0.36 eV at $\theta_e=-39°$. Instead of crossing the Fermi level, S_1 seems to turn downwards again beyond $\theta_e=-40°$, as expected from a fully occupied surface state band. Thus, in contrast to the two metallic surface state bands reported for the Au- and Cu-induced $\sqrt{21}\times\sqrt{21}$ surfaces,[4,6–8] our photoemission data only show one metallic surface band (S_4). To be able to compare with the surface that initially led to the interpretation of two metallic bands, we also show our Au-induced $\sqrt{21}\times\sqrt{21}$ spectra in Fig. 2(b). The two types of $\sqrt{21}\times\sqrt{21}$ surfaces show similar surface band structures near the Fermi level. The Au-induced $\sqrt{21}\times\sqrt{21}$ surface has an upward dispersing band S_1 and a S_4 band which crosses the Fermi level in quite close resemblance with the Ag case. The spectra of Fig. 2(b) are similar to the spectra presented in Refs. 6–8 for the same type of surface. The explanation to the different interpretations of the photoemission data can be found in the intensity behavior of the S_1 and S_4 surface states (S_1* and S_1' in Ref. 6). For the Ag-induced $\sqrt{21}\times\sqrt{21}$ surface one can clearly follow the S_1 band to its dispersion maximum at -39° and it is well separated from S_4. The relative intensity of the S_1 and S_4 states changes dramatically around that emission angle. The S_4 state becomes strong while the S_1 intensity quickly vanishes at higher emission angles. A very similar behavior is observed for the Au-induced $\sqrt{21}\times\sqrt{21}$ surface in Fig. 2(b). This rapid change in the intensities seems to be the reason why the S_1 state was believed to cross the Fermi level in the earlier studies. If just the strong peak is followed as one band it will give that impression. However, this leads to a clear discontinuity in

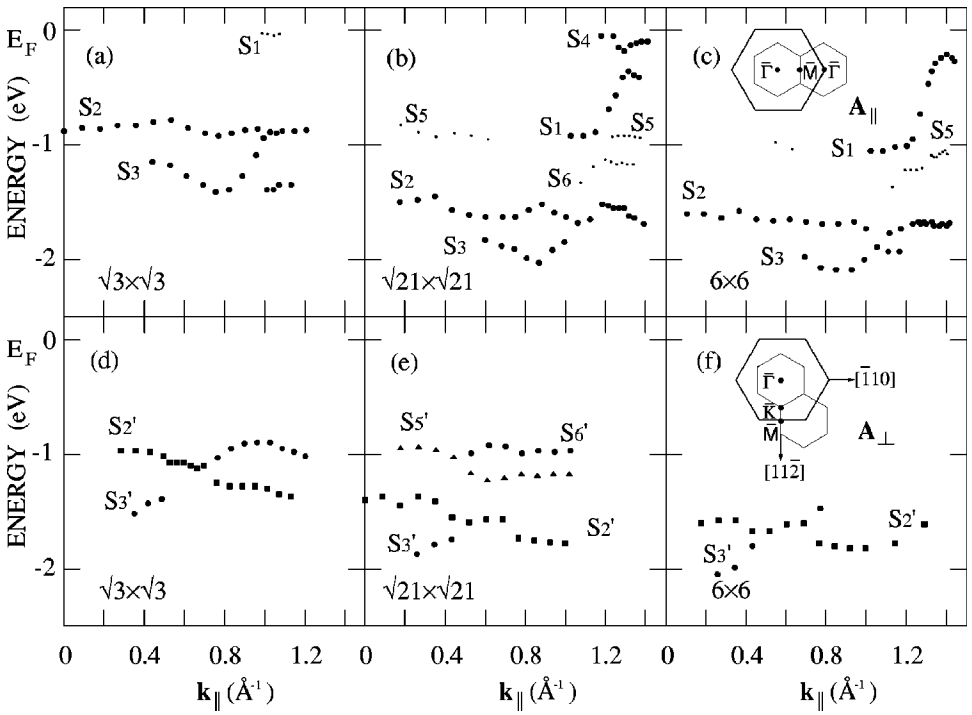

FIG. 3. Dispersions of the surface states on Ag/Si(111) along the $\bar{\Gamma}$-$\bar{M}$-$\bar{\Gamma}$ and $\bar{\Gamma}$-$\bar{K}$-$\bar{M}$ lines of the $\sqrt{3}\times\sqrt{3}$ SBZ (see inset). The dot size indicates the relative intensity of the different surface states. The projection of the light polarization vector on to the surface is either parallel to ($A_{\|}$) or perpendicular to ($A_{\perp}$) a given azimuthal direction during measurement. (a), (d) $\sqrt{3}\times\sqrt{3}$ surface; (b), (e) $\sqrt{21}\times\sqrt{21}$ surface; (c), (f) 6×6 surface.

the dispersion of the S_1* surface state at a $k_{\|}$ value of about 1.2 Å^{-1} (see Fig. 7 of Ref. 6). We can trace the jump in the dispersion curve to the quite different energy of S_1 at $-38°$ compared to S_4 at $-40°$ in Fig. 2(b). To conclude this part, we find that only one band (S_4) is metallic, while the S_1 band behaves as a fully occupied surface band.

Figure 2(c) shows a set of angle-resolved photoemission spectra obtained at 70 K from the 6×6 surface along the $\bar{\Gamma}$-$\bar{M}$-$\bar{\Gamma}$ line of the $\sqrt{3}\times\sqrt{3}$ SBZ. Four surface states were detected (S_1, S_2, S_3, and S_5). In contrast to the metallic character of the $\sqrt{21}\times\sqrt{21}$ surface, the 6×6 surface shows a semiconducting behavior, as evidenced by a clear gap of 0.2 eV with respect to E_F at $\theta_e=-41.5°$. In comparison to the $\sqrt{21}\times\sqrt{21}$ surfaces, we find that S_1 becomes significantly stronger and it shows a clear downwards dispersion above $\theta_e=-41.5°$, while the metallic band S_4 is missing. It is found that S_1 is located at -0.2 eV at $\theta_e=-41.5°$ and it disperses downwards to -1.05 eV at $\theta_e=-32°$. As can be seen from the spectra the addition of Ag atoms has a dramatic effect on the S_1 and S_4 bands. That is, S_1 becomes strong, while we find that S_4 vanishes for the 6×6 surface, resulting in the observed band gap. These results are consistent with our earlier observations on the $\sqrt{39}\times\sqrt{39}$ and 6×6 surfaces of Ag/Ge(111).[1]

Figure 3 shows a summary of the band structures of the three Ag-induced surfaces along the $\bar{\Gamma}$-$\bar{M}$-$\bar{\Gamma}$ and $\bar{\Gamma}$-$\bar{K}$-$\bar{M}$ lines. From these six panels, one can follow the changes observed for the different surface state bands. Since the $\sqrt{21}\times\sqrt{21}$ and 6×6 surfaces can be envisioned as adatom-induced superstructures on the $\sqrt{3}\times\sqrt{3}$ substrate, it is important to discuss the electronic structure on this basic surface. Earlier studies of the Ag/Si(111) $\sqrt{3}\times\sqrt{3}$ surface,[5,6] have reported three surface states S_1, S_2, and S_3, where S_1 is a metallic band. In the ideal HCT model of the 1 ML Ag/Si(111) $\sqrt{3}\times\sqrt{3}$ surface, there is an even number of valence electrons per unit cell. Thus the surface should have an inherently semiconducting character. One interesting observation from low temperature STM studies is that a highly mobile two-dimensional gas of extra Ag adatoms exists on the Ag/Si(111) $\sqrt{3}\times\sqrt{3}$ surface.[14] This could explain the origin of surface state S_1. The presence of these extra Ag adatoms, with their loosely bound *s* electrons, leads to a partial filling of the unoccupied surface state S_1 of the ideal $\sqrt{3}\times\sqrt{3}$ surface. Regarding our experimental results from the $\sqrt{3}\times\sqrt{3}$ surface, we want to point out that after the initial formation of the $\sqrt{3}\times\sqrt{3}$ surface there was always a significant intensity from the partially occupied, dispersing surface state (S_1) with a minimum energy of about 0.2 eV below the Fermi level. After the initial preparation the samples were carefully annealed up to 600 °C for several minutes in order to remove any surplus of Ag atoms. The result was that the S_1 peak shifted upwards to the Fermi level and it became almost extinct, which indicates that the $\sqrt{3}\times\sqrt{3}$ surface is intrinsically semiconducting. In a theoretical calculation of the $\sqrt{3}\times\sqrt{3}$ surface,[15] Aizawa *et al.* reported that a new inequivalent triangle (IET) model is energetically more favorable than the HCT model. The IET model predicts an asymmetry within the $\sqrt{3}\times\sqrt{3}$ unit cell, which has also been observed

by STM at 6 and 62 K.[14] As a consequence of the symmetry breaking, the S_2 and S_3 surface states, which are degenerate at the $\bar{K}$ point along the $\bar{\Gamma}$-$\bar{K}$-$\bar{M}$ line, were predicted to split. We have performed low temperature ARPES studies down to 70 K to investigate this effect. However, we did not find any splitting at the $\bar{K}$ point along the $\bar{\Gamma}$-$\bar{K}$-$\bar{M}$ line, and actually the 70 K valence band spectra are essentially the same as the 100 K and the room temperature spectra.

As shown by Fig. 3, there are clear similarities between the surface band structures of the $\sqrt{3}\times\sqrt{3}$, $\sqrt{21}\times\sqrt{21}$, and 6×6 surfaces. Figure 3(a) shows S_1 in an extreme energy position since the surface was annealed to remove any surplus of Ag adatoms. From our photoemission studies we find that the band minimum of S_1 shifts continuously downwards when more and more Ag is deposited on the $\sqrt{3}\times\sqrt{3}$ surface. It is therefore natural to suggest that S_1 of all surfaces have the same origins, since extra Ag does not destroy the $\sqrt{3}\times\sqrt{3}$ framework and the local atomic structure might still remain, according to previous STM studies.[11–13] As can be seen from Figs. 3(a) and 3(b), there is, however, a significant difference in energy of the S_1 minimum. Compared to the $\sqrt{3}\times\sqrt{3}$ surface the S_1 minimum has been pulled down by 0.86 eV, resulting in a completely occupied surface state band on the $\sqrt{21}\times\sqrt{21}$ surface. The same phenomenon occurs on the Au-induced $\sqrt{21}\times\sqrt{21}$ surface, i.e., the S_1 minimum is pulled down below the Fermi level as a small amount of Au is deposited on the $\sqrt{3}\times\sqrt{3}$ surface [Fig. 2(b)]. The S_2 and S_3 surface bands have also been pulled down (0.74 eV) compared to the $\sqrt{3}\times\sqrt{3}$ surface. Figures 3(d), 3(e), and 3(f), shows the dispersions of the S_2' and the S_3' states along the $\bar{\Gamma}$-$\bar{K}$-$\bar{M}$ line. These three panels clearly provide another piece of information about the different surface state bands. The downward displacement of the S_2' and S_3' surface bands on the $\sqrt{21}\times\sqrt{21}$ surface is very evident when comparing Figs. 3(d) and 3(e). The S_5' and S_6' surface bands which are present on the $\sqrt{21}\times\sqrt{21}$ surface appear at energies similar to S_2' and S_3' of the $\sqrt{3}\times\sqrt{3}$ surface [Fig. 3(d)]. This seems to indicate that the surface states of the $\sqrt{3}\times\sqrt{3}$ surface split into two groups due to a partial occupation of the Ag trimer sites. Therefore the S_4, $S_5(S_5')$ and $S_6(S_6')$ states may have the same origin as the initial S_1, $S_2(S_2')$, and $S_3(S_3')$ surface states of the $\sqrt{3}\times\sqrt{3}$ surface. Interestingly, on the 6×6 surface, the S_5' and S_6' surface state bands seem to be completely removed, and only the S_2' and S_3' surface states are left [Fig. 3(f)]. This is not too surprising, since further addition of Ag should continue to change the empty Ag trimer sites into sites occupied by Ag adatoms, resulting in a more or less complete conversion of the S_4, $S_5(S_5')$, and $S_6(S_6')$ states into the S_1, $S_2(S_2')$, and $S_3(S_3')$ surface states [Figs. 3(c) and 3(f)]. Once the surface state S_4 has been removed, then all surface states are below the Fermi level and the new semiconducting 6×6 surface is completed.

In conclusion, the surface electronic structures of four surfaces ($\sqrt{3}\times\sqrt{3}$, Au- and Ag-induced $\sqrt{21}\times\sqrt{21}$ and 6×6) have been investigated by ARPES. Two fully occupied surface state bands are found on the annealed $\sqrt{3}\times\sqrt{3}$ surface, which shows an intrinsic semiconducting character. Six surface state bands are found on the $\sqrt{21}\times\sqrt{21}$ surface. The surface electronic structures of the two $\sqrt{21}\times\sqrt{21}$ surfaces show clear similarities. We find, however, that only one surface band on the $\sqrt{21}\times\sqrt{21}$ surface is metallic in contrast to the two metallic bands discussed in earlier reports. The 6×6 surface has four surface state bands without any band crossing the Fermi level. The result is a semiconducting character of the 6×6 phase, with a gap of about 0.2 eV with respect to E_F. Thus, by depositing small amounts of Ag atoms on the $\sqrt{3}\times\sqrt{3}$ surface, the surface electronic structure shows an interesting change from a semiconducting to a metallic and back to a semiconducting state.

Support from the MAX-lab staff is gratefully acknowledged. This work was supported by the Swedish Natural Science Research Council.

*Electronic address: hazha@ifm.liu.se

[1] H.M. Zhang, T. Balasubramanian, and R.I.G. Uhrberg, Phys. Rev. B **63**, 195402 (2001).
[2] See, for example, Y.G. Ding, C.T. Chan, and K.M. Ho, Phys. Rev. Lett. **67**, 1454 (1991); **69**, 2452 (1992).
[3] Z.H. Zhang, S. Hasegawa, and S. Ino, Phys. Rev. B **52**, 10 760 (1995).
[4] S. Hasegawa, X. Tong, S. Takeda, N. Sato, and T. Nagao, Prog. Surf. Sci. **60**, 89 (1999).
[5] L.S.O. Johansson, E. Landemark, C.J. Karlsson, and R.I.G. Uhrberg, Phys. Rev. Lett. **63**, 2092 (1989); **69**, 2451 (1992).
[6] X. Tong, C-S. Jiang, and S. Hasegawa, Phys. Rev. B **57**, 9015 (1998).
[7] C.-S. Jiang, X. Tong, S. Hasegawa, and S. Ino, Surf. Sci. **376**, 69 (1997).
[8] S. Hasegawa, X. Tong, C.-S. Jiang, Y. Nakajima, and T. Nagao, Surf. Sci. **386**, 322 (1997).
[9] H. Aizawa and M. Tsukada, Phys. Rev. B **59**, 10 923 (1999).
[10] X. Tong, S. Hasegawa, and S. Ino, Phys. Rev. B **55**, 1310 (1997).
[11] J. Nogami, K.J. Wan, and X.F. Lin, Surf. Sci. **306**, 81 (1994).
[12] A. Ichimiya, H. Nomura, Y. Horio, T. Sato, T. Sueyoshi, and M. Iwatsuki, Surf. Rev. Lett. **1**, 1 (1994).
[13] X. Tong, Y. Sugiura, T. Nagao, T. Takami, S. Takeda, S. Ino, and S. Hasegawa, Surf. Sci. **408**, 146 (1998).
[14] S. Hasegawa, N. Shiraki, C.L. Petersen, P. Bøggild, T.M. Hansen, T. Nagao, and F. Grey, Jpn. J. Appl. Phys. **39**, 3815 (2000).
[15] H. Aizawa, M. Tsukada, N. Sato, and S. Hasegawa, Surf. Sci. **429**, L509 (1999).